Šimić, G., Mladinov, M., Šešo Šimić, Đ., Jovanov Milošević, N., Islam, A., Pajtak, A., Barišić, N., Sertić, J., Lucassen, P. J., Hof, P. R. Krušlin, B. (2008) *Abnormal motoneuron migration, differentiation, and axon outgrowth in spinal muscular atrophy.* Acta Neuropathologica, 115 (3). pp. 313-326.

The original publication is available at www.springelink.com

http://www.springerlink.com/content/q52u302730384870/

http://dx.doi.org/10.1007/s00401-007-0327-1

Goran Šimić[1], Mihovil Mladinov[1], Đurđica Šešo Šimić[2], Nataša Jovanov Miloševic[1], Atiqul Islam[3], Alen Pajtak[1], Nina Barišic[2], Jadranka Sertić[2], Paul Lucassen[4], Patrick R. Hof[5], Božo Krušlin[1]

Abnormal motoneuron migration, differentiation, and axon outgrowth in spinal muscular atrophy

[1]Department of Neuroscience, Croatian Institute for Brain Research, Medical School Zagreb, Salata 12, 10000 Zagreb, Croatia
[2]University Hospital Center Zagreb, Kispaticeva 12, 10000 Zagreb, Croatia
[3]Karolinska Institute, NOVUM B84, Huddinge 14 186, Stockholm, Sweden
[4]Centre for Neuroscience, Swammerdam Institute for Life Sciences, University of Amsterdam, Kruislaan 320, 1098 SM Amsterdam, The Netherlands
[5]Department of Neuroscience, Mount Sinai School of Medicine, One Gustave L. Lewy Place, Box 1065, New York, NY 10029, USA

Correspondence:
Goran Šimić, Department of Neuroscience, School of Medicine, Croatian Institute for Brain Research, Zagreb University, Croatia
Fax: +385-1-4596942, Phone: +385-1-4596807, E-mail: gsimic@hiim.hr

This work was supported by grants from the Ministry of Science, Education and Sports of Republic of Croatia (108-1081870-1884 to BK and 108-1081870-1942 to GŠ).

Abstract

The role of heterotopic (migratory) motoneurons (HMN) in the pathogenesis of spinal muscular atrophy (SMA) is still controversial. We examined the occurrence and amount of HMN in spinal cord tissue from eight children with SMA (six with SMA-I and two with SMAII). All affected subjects were carrying a homozygous deletion of exon 7 in the SMN1 gene. Unlike controls, virtually free from HMN, all SMA subjects showed a significant number of HMN at all levels of the spinal cord. Heterotopic neurons were hyperchromatic, located mostly in the ventral white matter and had no axon or dendrites. More than half of the HMN were very undifferentiated, as judged from their lack of immunoreactivity for NeuN and MAP2 proteins. Small numbers of more differentiated heterotopic neurons were also found in the dorsal and lateral white matter region. As confirmed by ultrastructural analysis, in situ end labeling (ISEL) and CD68 immunoreactivity, HMN in the ventral outflow were found to have no synapses, to activate microglial cells, and to eventually die by necrosis. An unbiased quantitative analysis showed a significant negative correlation between age of SMA subjects (a reflection of the clinical severity) and the number of HMN. Subjects who died at older ages had increased number of GFAP-positive astrocytes. Complementing our previous report on motoneuron apoptosis within the ventral horns in SMA, we now propose that abnormal migration, differentiation, and lack of axonal outgrowth may induce motoneuron apoptosis predominantly during early stages, whereas a slower necrosis-like cell death of displaced motoneurons which ‘‘escaped’’ apoptosis characterizes later stages of SMA.

Keywords motoneurons, migration, pathogenesis, spinal muscular atrophy, SMN1 gene

Introduction

Spinal muscular atrophy (SMA) is the second most common neuromuscular disease after muscular dystrophy, the second most common autosomal recessive disease after cystic fibrosis, and the leading known genetic cause of infant mortality [3]. SMA is characterized by the loss of spinal cord anterior horn (AH) neurons, hypotonia, and progressive denervation of skeletal muscles [13]. According to age at onset and severity, SMA is classified in several types that form the clinical spectrum. In SMA-I (Werdnig–Hoffmann disease, acute SMA), onset is usually before 9 months. Affected infants fail to achieve early motor milestones and are never able to sit. Death occurs within the first 2 years of life, usually due to the respiratory failure. Survival in SMA-I patients has increased in the recent years, in relation to better clinical care [36]. SMA-II is the intermediate or chronic infantile form, has an onset around 3–15 months. Children with SMA-II may sit but do not learn to ambulate. SMA-III (Kugelberg–Welander disease) has an onset between 1 and 15 years. These children are able to achieve walking and generally live into adulthood. SMA-IV is a rare adult form with onset after 30 years of age. SMA-III and SMA-IV are sometimes difficult to separate from long-duration forms of pure lower motor variant of amyotrophic lateral sclerosis (ALS) [51].

Nearly all SMA patients display homozygous deletions, rearrangements (gene conversions) or other mutations in the telomeric copy of the survival of motor neuron (SMN) gene on chromosome 5q13 [26]. Telomeric (SMN1) and centromeric (SMN2) genes differ by eight single nucleotide changes, two of which are in exons 7 and 8 [38]. The exon 7 C-to-T transition at codon 280 has been shown necessary and sufficient for skipping of exon 7 during alternative splicing [29]. Consequently, about 80–90% of SMN2 transcripts lack exon 7 and their dysfunctional protein product is insufficient to compensate for the loss of SMN1 protein [35]. Higher number of SMN2 copies (due to gene conversion events) has been linked to the less severe SMA types [14, 31]. However, as even diseased siblings with the same number of SMN2 genes can have different SMA phenotypes, SMN locus itself cannot explain the genetic basis for phenotypic variability of SMA [12]. As many reports show, the clinical severity of the disease can be modified by the extent of deletion at SMN locus [5] encompassing other phenotypic modifier genes such as neuronal apoptosis inhibitory protein (NAIP) [40, 45] and H4F5 gene [23, 43].

The SMN protein is a unique and poorly known molecule with many binding partners. SMN is found to be most abundant in the cytoplasm and nucleus of alpha motoneurons [1, 2, 53]. It is involved in various cellular processes, of which four seem to be best documented: assembly of spliceosomal small nuclear ribonucleoproteins (snRNPs) and pre-mRNA processing (splicing) [16], activation of transcription/translation [6], apoptosis [21, 22, 28, 42, 54], and axonal transport [2, 8, 19, 34, 37, 39, 46]. Which of these functions is most important for the pathogenesis of SMA is not clear.

Together with the degeneration and loss of the AH cells (alpha and gamma motoneurons as well as interneurons), ‘‘empty cell beds’’ and glial cell bundles of ventral spinal roots that were originally described by Werdnig in [50], heterotopic (migratory) motoneurons (HMN) are postulated to be one of the hallmark neuropathological findings in SMA [9]. However, the importance of this phenomenon in the pathogenesis of SMA has been largely neglected in both classical [24] and more contemporary studies [15, 33, 51]. Therefore, we re-examined the occurrence,

quantity, and ultrastructural morphology of HMN in children with clinically, pathologically, and genetically confirmed SMA.

Materials and methods

We investigated six children with SMA-I (three males, three females) and two children with SMA-II (two females), as well as five control subjects (two males, three females) who had no neurological disorder and died from either congenital heart disease or peritonitis. Five SMA-I and control cases were included in our previous study where we analyzed presence of apoptosis in gray matter of the AHs of the spinal cord [48]. The diagnosis of SMA was made on the basis of clinical findings (progressive muscle weakness and hypotonia), electromyoneurography, muscle biopsy, and was confirmed by genetic analysis of blood samples. Genotyping was performed using PCR amplifying exons 7 and 8 of the SMN1 gene, and exon 5 of the NAIP gene, as described previously [45, 48]. All eight affected subjects were carrying homozygous deletion of exon 7 in the SMN1 gene. Brain and muscle tissues were obtained at routine autopsies with informed consent from the families. Postmortem intervals varied from 4 to 7 h.

After formalin fixation, affected muscle tissue was stained using routine hematoxylin and eosin (H–E) staining. Following fixation in 4% formaldehyde in phosphate buffer saline (PBS, pH = 7.4) for several days to 4 weeks, each spinal cord was cut in the rostrocaudal direction in several slabs. Slabs were dehydrated through a graded series of ethanol solutions, cleared in toluene, embedded in paraffin (Histowax, Jung, Nussloch, Germany) and serially cut in 15-lm-thick sections. After deparaffinization in xylene, the sections were collected in 70% ethanol, put in 50% and then in 5% ethanol, then put in distilled water, and finally in a staining solution, which consisted of one part of 0.5% cresyl violet in distilled water mixed with four parts of distilled water. Upon achieving adequate staining, the sections were placed in distilled water, then dehydrated through a graded series of alcohol solutions and finally in ether–ethanol solution (two parts of ether and one part of 100% ethanol), rinsed with xylene, and mounted.

To confirm further that the observed heterotopic cells are truly neurons, we used NeuN and MAP2 immunocytochemistry. NeuN is a phosphoprotein that serves for identification of postmitotic neurons. Depending on the isoform (46 or 48 kDa), it can be localized either in the neuronal nuclei (in areas of low chromatin density) or in the neuronal cytoplasm [27]. MAP2 is a microtubuleassociated protein also specifically expressed in neuronal cells. To eliminate endogenous peroxidases and nonspecific staining, tissue sections were pretreated for 20 min in 0.3% hydrogen peroxide in the mixture of methanol and redistillated water (3:1), washed (3 9 10 min in PBS) and incubated with blocking solution (PBS containing 3% BSA and 0.5% Triton X-100, all from Sigma, St. Louis, MO, USA) for 2 h at room temperature. The sections were then incubated at 4ºC for 18 h with a monoclonal anti-neuronalnuclei antibody (NeuN, MAB377, clone A60, from Chemicon, Temecula, CA, USA) diluted in blocking solution (1:1,000) or anti-MAP2 antibody at 4ºC overnight (Sigma, St. Louis, MO, USA, diluted 1:1,000), washed again and incubated with secondary biotinylated antimouse antibody in blocking solution (1:200) for 1 h at room temperature (Vectastain ABC kit, Vector Laboratories, Burlingame, USA). Following another washing, the sections were incubated in Vectastain ABC reagent (streptavidin-peroxidase complex) for 1 h at room temperature and washed. Finally,

peroxidase activity was visualized using Ni-3,30-diaminobenzidine (DAB) (Sigma). In control sections, the primary antibody was omitted. The sections were washed in PBS, air-dried, dehydrated in a graded series of alcohol, cleared in xylene, and coverslipped with Histamount (National Diagnostics, Atlanta, GA, USA). Immunohistochemistry for glial fibrillary acidic protein (GFAP) was performed using an anti-cow GFAP monoclonal rabbit IgG (Dako, Copenhagen, Denmark) in dilution 1:200, whereas macrophage/microglial marker CD68 was revealed using a rat anti-mouse CD68 antibody (Serotec Ltd, Kidlington, Oxford, UK, cat. No. MCA1957) in 1:80 dilution. Before immunohistochemistry, most slides were prestained with a Nissl stain to find which of them contained heterotopic neurons. Only those sections which contained HMN were destained from cresyl violet using graded alcohol solutions (from absolute to 50% solution and then phosphate buffer) and then incubated with primary antibodies. It should be noted that some of the cells, notably ependymal cells around the central canal, remained filled with cresyl-violet stain (purple color), which did not mix with specific immunoreactivity visualized by DAB (dark brown to black product) (as can be seen e.g., on Figs. 6 and 7).

For in situ end labeling (ISEL), sections were deparaffinized in xylene and hydrated to 50% ethanol in distilled water, preincubated with proteinase K (PK) buffer (10 mM Tris/HCl, 2.6 mM CaCl2, pH 7.0), and incubated with 5 μg/ml PK (Sigma, Zwijndrecht, The Netherlands),as described earlier [30, 48, 52]. Upon washing in distilled water, sections were incubated with terminal transferase (TdT) buffer (0.2 M sodium cacodylate, 0.025 M Tris/HCl in 0.25 mg/ml bovine serum albumine (BSA), pH 6.6) for 15 min at room temperature and then for 60 min at 37ºC with a reaction mixture that contained 0.2 ll TdT (terminal transferase) (Boehringer Mannheim, Almere, The Netherlands)/100 ll reaction mixture and 1.0 ll biotin-16-dUTP (Boehringer Mannheim)/100 ll reaction mixture and cobalt chloride (25 mmol; 5% of the final volume). Incorporation of labeled oligonucleotides was ended by rinsing the sections in distilled water and PBS. Endogeneous peroxidase activity was blocked with 0.01% H2O2 in PBS for 20 min at room temperature, after which the sections were washed in PBS, preincubated with PBS/1% BSA for 15 min, and incubated with peroxidase-conjugated avidin (ABC Elite kit, Vector Laboratories) 1:1000 in PBS/1% BSA overnight at 4ºC. Following washing in PBS, labeled DNA was visualized by incubation with 0.5 μg /ml diaminobenzidine (DAB) (Sigma) in 0.05 M Tris/HCl (pH 7.5) with 0.02% H2O2 for exactly 12 min. Color development was stopped by washing in distilled water. Positive controls from rat prostate 3 days after castration were included in every assay [52].

After fixation in 4% formaldehyde and 1.5% glutaraldehyde in PBS, selected slices of spinal cords were separated under a dissecting microscope and cut transversely on an ultramicrotome into semithin sections and stained with toluidine blue. Upon light-microscopic examination, ultrathin sections were cut for electron microscopy. The sections were rinsed in 0.1 MNa–cacodylate buffer, postfixed at 4ºC for 2 h in 1% OsO4 in 0.1 M Na–cacodylate buffer, dehydrated in a graded series of ethanol, and embedded in LX112 acetone. The specimens were analyzed on a Philips 420 electron microscope at 80 kV.

Estimates of number of heterotopic (migratory) neurons were unbiasedly obtained by the physical disector method [20] using an Olympus Provis AX70 microscope equipped with a Nikon DXM 1200 camera attached to the computer. Upon a random start, every 6 and 7th section were systematically sampled and used for quantification. Statistical analysis was carried out using Statistica 7.0 software (StatSoft 2006, Tulsa, OK) and included Pearson's coefficient of correlation and regression analysis.

We investigated six children with SMA-I (3 males, 3 females) and two children with SMA-II (2 females), as well as five control subjects (2 males, 3 females) who had no neurological disorder and died from either congenital heart disease or peritonitis. Five SMA-I and control cases were included in our previous study where we analyzed presence of apoptosis in gray matter of the anterior horns of the spinal cord [46]. The diagnosis of SMA was made on the basis of clinical findings (progressive muscle weakness and hypotonia), electromyoneurography, muscle biopsy, and was confirmed by genetic analysis of blood samples. Genotyping was performed using PCR amplifying exons 7 and 8 of the SMN1 gene, and exon 5 of the NAIP gene, as described previously [43, 46]. All eight affected subjects were carrying homozygous deletion of exon 7 in the SMN1 gene. Brain and muscle tissues were obtained at routine autopsies with informed consent from the families. Postmortem time varied from 4 to 7 hours.

Upon formalin fixation, affected muscle tissue was stained using routine hematoxylin and eosin (H-E) staining. Following fixation in 4% formaldehyde in phosphate buffer saline (PBS, pH = 7.4) for several days to 4 weeks, each spinal cord was cut in the rostrocaudal direction in several slabs. Slabs were dehydrated through a graded series of ethanol solutions, cleared in toluene, embedded in paraffin (Histowax, Jung, Nussloch, Germany) and serially cut in 15-μm-thick sections. After deparaffinization in xylene, the sections were collected in 70% ethanol, put in 50% and then in 5% ethanol, then put in distilled water, and finally in a staining solution, which consisted of 1 part of 0.5% cresyl violet in distilled water mixed with 4 parts of distilled water. Upon achieving adequate staining, the sections were placed in distilled water, then dehydrated through a graded series of alcohol solutions and finally in ether-ethanol solution (2 parts of ether and 1 part of 100% ethanol), rinsed with xylene, and mounted.

To confirm further that the observed heterotopic cells are truly neurons, we used NeuN and MAP2 immunocytochemistry. NeuN is a phosphoprotein that serves for identification of postmitotic neurons. Depending on the isoform (46 or 48 kDa), it can be localized either in the neuronal nuclei (in areas of low chromatin density) or in the neuronal cytoplasm [26]. MAP2 is a microtubule-associated protein also specifically expressed in neuronal cells. To eliminate endogenous peroxidases and non-specific staining, tissue sections were pretreated for 20 min in 0.3% hydrogen peroxide in the mixture of methanol and redistillated water (3:1), washed (3 x 10 min in PBS) and incubated with blocking solution (PBS containing 3% BSA and 0.5% Triton X-100, all from Sigma, St. Louis, MO, USA) for 2 hours at room temperature. The sections were then incubated at 4°C for 18 hours with a monoclonal anti-neuronal-nuclei antibody (NeuN, MAB377, clone A60, from Chemicon, Temecula, CA, USA) diluted in blocking solution (1:1,000) or anti-MAP2 antibody at 4°C overnight (Sigma, St. Louis, MO, USA, diluted 1:1,000), washed again and incubated with secondary biotinylated anti-mouse antibody in blocking solution (1:200) for 1 hour at room temperature (Vectastain ABC kit, Vector Laboratories, Burlingame, USA). Following another washing, sections were incubated in Vectastain ABC reagent (streptavidin-peroxidase complex) for 1 hour at room temperature and washed. Finally, peroxidase activity was visualized using Ni-3,3'-diaminobenzidine (DAB) (Sigma). In control

sections the primary antibody was omitted. The sections were washed in PBS, air-dried, dehydrated in a graded series of alcohol, cleared in xylene and cover-slipped with Histamount (National Diagnostics, Atlanta, GA, USA). Immunohistochemistry for glial fibrillary acidic protein (GFAP) was performed using anti-cow GFAP monoclonal rabbit IgG (Dako, Copenhagen, Denmark) in dilution 1:200, whereas CD68 antigen was revealed using rat anti-mouse CD68 antibody from Serotec Ltd (Kidlington, Oxford, UK, cat. No. MCA1957) in 1:80 dilution. Before immunohistochemistry, most slides were pre-stained by Nissl stain to find which of them contain heterotopic neurons. Only those sections which contained HMN were destained from cresyl violet using graded alcohol solutions (from absolute to 50% solution and then phosphate buffer) and then incubated with primary antibodies. It should be noted that some of the cells, notably ependymal cells around the central canal, remained filled with cresyl-violet dye (purple color), which should not be mixed with specific immunoreactivity visualized by DAB (dark brown to black product) (as can be seen e.g. on Figs. 6 and 7).

For ISEL (*in situ* end labeling), sections were deparaffinized in xylene and hydrated to 50% ethanol in distilled water, preincubated with proteinase K (PK) buffer (10 mM Tris/HCl, 2.6 mM $CaCl_2$, pH 7.0), and incubated with 5 μg/ml PK (Sigma, Zwijndrecht, The Netherlands), as described earlier [29, 46, 50]. Upon washing in distilled water, sections were incubated with terminal transferase (TdT) buffer (0.2 sodium cacodylate, 0.025 M Tris/HCl in 0.25 mg/ml bovine serum albumine (BSA), pH 6.6) for 15 minutes at room temperature and then for 60 minutes at 37°C with a reaction mixture that contained 0.2 μl TdT (terminal transferase) (Boehringer Mannheim, Almere, The Netherlands)/100 μl reaction mixture and 1.0 μl biotin-16-dUTP (Boehringer Mannheim)/100 μl reaction mixture and cobalt chloride (25 mmol; 5% of the final volume). Incorporation of labeled oligonucleotides was ended by rinsing the sections in distilled water and PBS. Endogeneous peroxidase activity was blocked with 0.01% H_2O_2 in PBS for 20 minutes at room temperature, after which the sections were washed in PBS, preincubated with PBS/1% BSA for 15 minutes, and incubated with peroxidase-conjugated avidin (ABC Elite kit, Vector Laboratories) 1:1000 in PBS/1% BSA overnight at 4°C. Following washing in PBS, labeled DNA was visualized by incubation with 0.5 μg/ml diaminobenzidine (DAB) (Sigma) in 0.05 M Tris/HCl (pH 7.5) with 0.02% H_2O_2 for exactly 12 minutes. Color development was stopped by washing in distilled water. Positive controls from rat prostate 3 days after castration were included in every assay [50].

After fixation in 4% formaldehyde and 1.5% glutaraldehyde in PBS, selected slices of spinal cords were separated under a dissecting microscope and cut transversely on an ultramicrotome into semi-thin sections and stained with toluidine blue. Upon light-microscopic examination, ultra-thin sections were cut for electron microscopy. The sections were rinsed in 0.1 M Na-cacodylate buffer, postfixed at 4°C for 2 hours in 1% OsO_4 in 0.1 M Na-cacodylate buffer, dehydrated in a graded series of ethanol, and embedded in LX112 acetone. The specimens were analyzed on a Philips 420 electron microscope at 80 kV.

Estimates of number of heterotopic (migratory) neurons were unbiasedly obtained by the physical disector method [19] using an Olympus Provis AX70 microscope equipped with a Nikon DXM 1200 camera attached to the computer. Upon a random start, every 6^{th} and 7^{th} section were systematically sampled and used for quantification. Statistical analysis was carried out using Statistica 7.0 software (StatSoft 2006, Tulsa, OK) and included Pearson's coefficient of correlation and regression analysis.

Results

Affected muscle tissue showed typical pathological changes consistent with the diagnosis of SMA. In SMA-I and SMA-II subjects many sections contained HMN that were never observed in control subjects. Most of the heterotopic motoneurons were located outside the AH in the white matter of the anterior part of the spinal cord (ventral outflow) (Fig. 1a). They were almost always oval-shaped (undifferentiated) and without axonal or dendritic processes (Fig. 1b). In comparison to the motoneurons that remained in the gray matter of the AHs, which were always well-differentiated and frequently chromatolytic (‘‘ballooned motoneurons’’; Fig. 1c), the heterotopic motoneurons were never chromatolytic, but always more or less hyperchromatic (Figs. 1b, 2a, b, 3b; for more detailed microscopic and ultrastructural appearance of chromatolytic neurons see [48]). Majority of HMN were large or very large cells with diameter greater than 25 lm, while about 5–10% of the displaced cells had relatively small size—approximately three to five times smaller in crosssectional profile than large cells (e.g., several such cells can be seen on Fig. 6c). Many of the observed heterotopic motoneurons were found to accumulate at the anterior rim of the spinal cord (Figs. 2a, b, 6, 7). In some sections, particularly those of younger SMA subjects, we observed more than 10 heterotopic motoneurons aligned at the front wall of the spinal cord or outside the spinal cord (Fig. 2c). In Nissl-stained sections, some heterotopic motoneurons were found to strongly activate microglia-like cells (Figs. 1b, 3b–d). Late stages of neuronophagia of HMN by activated microglia-like cells are illustrated in Fig. 3c and d. Sometimes the heterotopic motoneurons went far into the anterior spinal root (Fig. 4a–d). In these cases, activation of glial cells seemed to be even stronger (Fig. 4a–d). However, when taking into account all of the sections analyzed, degenerative changes of HMN and their heterophagic elimination were found to occur in a relatively small (\5%) proportion of the total population of the observed displaced neurons. Abnormally migrating cells were occasionally seen in the ‘‘dorsal outflow,’’ dorsal to the Clarke’s column (Fig. 5a, b). Unlike HMN in the ventral outflow, which were always morphologically undifferentiated (i.e., without axon and dendrites), these heterotopic neurons were usually well differentiated (Fig. 5c, d). Rarely, we also observed abnormally migrating neurons in the lateral part of the spinal cord which were even less numerous and more differentiated.

NeuN and MAP2 immunocytochemistry showed that less than a half of the heterotopic cells are matured neurons (Figs. 6 and 7). In contrast, nondisplaced neurons within the AHs demonstrated normal development and differentiation of dendritic structures (Fig. 7a, b). The numbers of NeuN and MAP2 immunolabeled heterotopic neurons varied from case-to-case and from slide-to-slide, but it was our impression that nearly 50% of HMN in the ventral white matter were NeuN-positive, whereas only about 25% were positive for MAP2 (Figs. 6 and 7).

Immunohistochemistry for macrophage/microglial marker CD68 confirmed our observations made on Nissl stained sections in that degenerated HMN were found to be eliminated by CD68-positive activated microglia cells (Fig. 8). It should be however noted that besides CD68-positive microglia directly involved in phagocytosis of HMN, there were often many positive cells along the pathway of abnormal migration of HMN (some of which are denoted by arrowheads in Fig. 8b and c). In controls, we did not find any CD68-positive cells except sporadically in association with blood vessels and within central canal (Fig. 8g).

Unlike the situation within the ventral horns, where substantial quantities of ISEL-positive microglial cells were regularly seen in close proximity to apoptotic and degenerating neurons (Fig. 9a, b), ISEL-positive microglial cells were also seen in the ventral outflow of the spinal cord (Fig. 9c). A few disintegrating HMN showed positive ISEL staining (Figs. 4e, 9d, e). However, because ISEL staining in fact recognizes DNA damage associated with both apoptosis and necrosis, on the basis of the morphological appearance (membrane breaks, cellular disintegration, prominent heterophagic elimination), we concluded that HMN are dying by a slow, necrotic type of cell death.

Immunoreactivity for GFAP showed large inter- and intrasubject variability. Together with astrocytes, in both normal controls and SMA subjects, GFAP staining was also associated with immunoreactivity of small size capillaries (with perivascular staining belonging to astrocytes). However, it was our general impression that SMA subjects differ from controls and among themselves in the following two ways. First, in contrast to normal controls, where GFAP immunoreactivity consisted of lightly and evenly distributed immunoreactivity of small astrocytes within the white matter fiber tracts, many sections from SMA subjects revealed the presence of medium and large astrocytes in close proximity to ''empty cell beds'' within the ventral horns of the spinal cord (Fig. 9f, g). Second, it appeared that subjects who died at an older age contained increased number of GFAP-positive astrocytes (Fig. 9h) (no quantification was made). We found no GFAP-positive astroglia around HMN (Fig. 9i).

Unlike control tissues, in which we were unable to demonstrate any necrotic motoneurons, electron microscopic analysis in materials from children with SMA revealed some oval shaped HMN in various stages of degeneration (Fig. 10a, b). The observed changes included breakdown of the plasma membrane, vacuolization of cytoplasmic organelles, and loss of structure, which are consistent with necrotic cell death type [10, 17]. In contrast to normal motoneurons, heterotopic motoneurons contained no ultrastructurally identifiable synapses. Microglial cells were seen in the vicinity of degenerating heterotopic motoneurons (Fig. 10a), as judged from their small size, irregular shape, and clumping of the chromatin along the inner side of the nuclear envelope.

Out of 3,307 sections sampled with physical disectors, 420 sections contained altogether 597 heterotopic motoneurons. The estimated total number of heterotopic motoneurons for each subject is shown in Fig. 11. The number of migratory motoneurons could be best described by an exponential regression equation: number of migratory motoneurons = $1240 * e^{0.07 * \text{age in months}}$. The quantitative results showed a significant negative correlation between age of SMA subjects (which is a reflection of the clinical severity of the disease), and the number of heterotopic motoneurons (Pearson's coefficient of correlation $r = -0.64$, $p = 0.04$).

Discussion

Our results clearly demonstrate that a significant number of motor neurons in the spinal cord of children with SMA-I and SMA-II, but not in controls, aberrantly migrate toward the ventral spinal roots. Suprisingly, half or more of these HMN are very undifferentiated. Absence of proteins specific for matured neurons such as NeuN and MAP2 suggests ''arrested'' differentiation of HMN in a very early stage of development. To explore this issue further, doublestaining and expression of other markers of differentiation such as b-III-tubulin should be investigated. Most of HMN

are found to look morphologically healthy and remain present at the anterior rim of the spinal cord or within ventral spinal roots, while a very small proportion of these cells has been found in various stages of, presumably necrotic, degeneration. Since we observed just the endstage of the disease at autopsy, it is logical to assume that many more displaced cells were present in the tissue during earlier stages of the disease. Fewer but more differentiated migrating neurons are also present in the dorsal and lateral white matter region of the spinal cord. This finding contradicts most of the earlier studies, except perhaps that of Chou and Wang [9], and suggests that abnormal migration may underlie the pathogenesis of SMA.

We demonstrated previously apoptotic motoneuron death in a small proportion of the remaining spinal motoneurons in children with SMA-I [48]. As apoptotic neurons could be found only inside the gray matter of the AHs [48], we concluded that observed and here described abnormally migrated motoneurons somehow escaped apoptosis. Ultrastructural and ISEL analysis demonstrates that some of such heterotopic motoneurons in the spinal cord of children with SMA die by necrotic cell death [10, 17]. As postmortem delays were relatively short (4–7 h), we believe that the degenerative changes described were not caused by postmortem artifacts. Although phagocytosis is not limited to necrotic cells, given the non-controlled leakage of various cellular components into the neuropil during necrosis, one would expect that a phagocytic response may be more prominent and variable than when apoptosis or autophagic cell death occur, which are generally more silent and not expected to trigger a strong response. We therefore think that the necrotic mechanism of cell death is further supported by evidence of phagocytosis of necrotic HMN by microglial cells, which was confirmed by CD68 immunolabeling.

In our view, there are two possible explanations for finding of diffuse cytoplasmic ISEL staining of microglia in some sections (Fig. 9). First, in view of their role in phagocytosis, ISEL signal in the cytoplasm could represent the remnants of DNA of dying neighboring cells or neurons that had to be cleared and have been taken up by microglia. As such, this pattern does not necessarily confirm that the microglia cell itself is dying. Second, we do not know whether the cell death process of a microglia cell is identical to that of a neuron. Therefore, depending on the stage of the death process, fragmented DNA of the microglia cell nucleus itself can also leak into the cytoplasm, which is seen in some in vitro preparations and would explain the present pattern as well. Ultrastructural morphological features of activated microglial cells (irregular shape and clumping of the chromatin along the inner side of the nuclear envelope, Fig. 10) further suggest that these cells are undergoing apoptosis. Apoptosis in this case probably reflects a physiological mechanism by which excess amounts of microglial cells are eliminated. Our observation that AHs are usually more immunoreactive for GFAP than posterior horns is in accordance with increased content of GFAP found on two-dimensional electrophoretic gel from SMA-I spinal cord samples [4].

It is difficult to estimate how many of the apoptotic motoneurons within the gray matter (see [48]) are actually dying due to aberrant migration, but we speculate that abnormal migration may induce motoneuron apoptosis of a small population of motoneurons within the gray matter in early stages of the disease and necrosis of a larger population of heterotopic motoneurons at later stages of SMA. In comparison to rapid intrauterine changes (presumably of apoptotic origin), these findings therefore imply a relatively slower mode of necrotic degeneration of displaced AH neurons after birth, in SMA children. Nevertheless, how exactly mutations in the SMA-determining gene SMN1 and other candidate disease-modifying genes and their

protein products cause abnormal migration and cell death remains to be elucidated. The recent findings of interaction and translocation of SMN protein and b-actin mRNA to axons and growth cones [39] as well as the asymmetric SMN protein staining demonstrated in the germinative neuroepithelium [19] strongly support a specific role of SMN protein in motoneuron axonogenesis, migration, and differentiation. This role seems to be relevant for SMA pathogenesis, but independent of snRNP biosynthesis [8].

Although deletions or mutations in the SMN1 gene are most highly correlated with SMA, it is not clear to what extent SMN2, NAIP or other genes influence the SMA phenotype, or whether some of SMA patients actually have functional copies of both SMN1 and NAIP. Due to the facts that large scale deletions and rearrangements of the 5q13 region are specific for more severe (SMA-I) cases [5] and that we found a higher number of motoneurons undergoing abnormal migration in these cases, it is reasonable to speculate that in more severe SMA cases other genetic changes in the vicinity of SMN locus might influence the course of the disease. For example, it is not clear whether irregularly high transcription of the variable number of cadherin12 pseudogenes in the SMN region somehow relates to the pathogenesis of SMA [44].

As no sensory involvement can be found clinically, it is less widely recognized that the pathology of SMA may include cells other than those in the AHs. Namely, more subtle neuropathological changes in SMA have been already described in the lateral thalamic nucleus, cerebellar and brainstem nuclei, the nucleus of Clarke, and in dorsal root ganglia [32, 47]. Our observations of aberrant migration in the dorsal and lateral part of spinal cord white matter confirm and extend some of these earlier observations and support the idea that SMA is a multisystemic disease involving both motor and sensory systems. These, somewhat surprising, findings may be important for future molecular and cellular studies of this enigmatic disorder.

We believe that our results provide some key evidence for resolving important and unanswered questions from previous investigations. For example, in a classical work on glial cell bundles in SMA-I Ghatak concluded: ‘‘…The present observations suggest that such glial migration, although apparently unique in Werdnig–Hoffmann disease, is a secondary phenomenon and fails to resolve the issue as to whether neuronal degeneration or an injury to the nerve roots is the primary event in this disorder’’ [18]. On the basis of our findings described here, we think that abnormal migration is the primary pathogenetic event in SMA, which causes (attracted) glial cells to follow displaced neurons thus forming glial cell bundles of ventral spinal roots. In fact, abnormal migration may be responsible for all major neuropathological features of SMA, including the loss of the AH cells and ‘‘empty cell beds.’’

Similarly to SMA, there is a still ongoing controversy regarding the origin, presence, and role of HMN in the spinal cord of ALS patients [25, 33, 41]. Besides families in which SMA and ALS coexist [7], it has been shown that SMN genotypes that produce less SMN protein [49] or have different SMN1 gene copy numbers [11] increase the risk of sporadic ALS or duration of ALS evolution. In this context, the findings described in the present study may also be relevant for future research on heteterotopic neurons in the pathogenesis of ALS.

In conclusion, we convincingly demonstrated, albeit in a relatively small number of SMA subjects, that abnormal migration, differentiation, and axon outgrowth may represent pathogenetic mechanisms of this devastating disease. However, how exactly mutations in SMA gene SMN1 and other disease-modifying genes and their protein products prevent motoneuron axonogenesis and cause aberrant migration remains to be elucidated. Given some possible genetic interactions between SMA and the risk for

developing ALS, our findings may also bear considerable relevance for future research on axonopathy and heterotopic neurons in the pathogenesis of ALS.

Acknowledgements

We thank Z. Cmuk, D. Budinscak, B. Popovic (Department of Neuroscience, Croatian Institute for Brain Research), D. Poljan (Department of Pathology, Medical School Zagreb) and I. Jusinsky (Clinical Research Center – Electron Microscopy Unit, Huddinge University Hospital, Karolinska Institute, Stockholm) for excellent technical help.

References

1. Battaglia G, Princivalle A, Forti F, Lizier C, Zeviani M (1997) Expression of the SMN gene, the spinal muscular atrophy determining gene, in the mammalian central nervous system. Hum Mol Genet 6:1961–1971
2. Be´chade C, Rostaing P, Cisterni C, Kalisch R, La Bella V, Pettmann B, Triller A (1999) Subcellular distribution of SMN protein: possible involvement in nucleoplasmic and dendritic transport. Eur J Neurosci 11:293–304
3. Botta A, Tacconelli A, Bagni I, Giardina E, Bonifazi E, Pietropolli A, Clementi M, Novelli G (2005) Transmission ration distortion in the spinal muscular atrophy locus: data from 314 prenatal tests. Neurology 65:1631–1635
4. Brock TO, McIlwain DL (1984) Astrocytic proteins in the dorsal and ventral roots in amyotrophic lateral sclerosis and Werdnig–Hoffmann disease. J Neuropahol Exp Neurol 43:609–619
5. Burlet P, Burglen L, Clermont O, Lefebvre S, Viollet L, Munnich A, Melki J (1996) Large scale deletions of the 5q13 region are specific to Werdnig–Hoffmann disease. J Med Genet 33:281–283
6. Campbell L, Hunter KM, Mohaghegh P, Tinsley JM Brasch MA, Davies KE (2000) Direct interaction of SMN with dp103, a putative RNA helicase: a role for SMN in transcription regulation? Hum Mol Genet 9:1093–1100
7. Camu W, Billiard M (1993) Coexistence of amyotrophic lateral sclerosis and Werdnig–Hoffmann disease within a family. Muscle Nerve 16:569–570
8. Carrel TL, McWhorter ML, Workman E, Zhang H, Wolstencroft EC, Lorson C, Bassell GJ, Burghes AH, Beattie CE (2006) Survival motor neuron function in motor axons is independent of functions required for small nuclear ribonucleoprotein biogenesis. J Neurosci 26:11014–11022
9. Chou SM, Wang HS (1997) Aberrant glycosylation/phoshorylation in chromatolytic motoneurons of Werdnig–Hoffmann disease. J Neurol Sci 152:198–209
10. Clarke PGH (1990) Developmental cell death: morphological diversity and multiple mechanisms. Anat Embryol 181:195–213
11. Corcia P, Camu W, Halimi JM, Vourc'h P, Antar C, Vedrine S, Giraudeau B, de Toffol B, Andres CR (2006) SMN1 gene, but not SMN2, is a risk factor for sporadic ALS. Neurology 67:1147–1150
12. Cusco´ I, Barcelo´ MJ, Rojas-Garcı´a R, Illa I, Gamez J, Cervera C, Pou A, Izquierdo G, Baiget M, Tizzano EF (2006) SMN copy number predicts acute or chronic spinal muscular atrophy but does not account for intrafamilial variability in siblings. J Neurol 253:21–25
13. Dubowitz V (1995) Disorders of the lower motor neuron, the spinal muscular atrophy. In: Dubowitz V (ed) Muscle disorders in childhood. Saunders, London, pp 325–369
14. Feldko¨ tter M, Schwarzer V, Wirth R, Wienker TF, Wirth B (2002) Quantitative analyses of SMN1 and SMN2 based on realtime light-cycler PCR: fast and highly reliable carrier testing and prediction of severity of spinal muscular atrophy. Am J Hum Genet 70:358–368
15. Fidzianska A, Rafalowska J (2002) Motoneuron death in normal and spinal muscular atrophy-affected human fetuses. Acta Neuropathol 104:363–368

16. Fischer U, Liu Q, Dreyfuss G (1997) The SMN-SIP1 complex has an essential role in spliceosome biogenesis. Cell 90:1023–1029
17. Galluzzi L, Maiuri MC, Vitale I, Zischka H, Castedo M, Zitvoogel L, Kroemer G (2007) Cell death modalities: classification and pathophysiological implications. Cell Death Diff 14:1237–1243
18. Ghatak NR (1978) Spinal roots in Werdnig–Hoffmann disease. Acta Neuropathol 41:1–7
19. Giavazzi A, Setola V, Simonati A, Battaglia G (2006) Neuronalspecific roles of the survival motor neuron protein: evidence from survival motor neuron expression patterns in the developing human central nervous system. J Neuropathol Exp Neurol 65:267–277
20. Gunthinas-Lichius O, Mockenhaupt J, Stennert E, Neiss WF (1993) Simplified nerve cell counting in the rat brainstem with the physical disector using a drawing microscope. J Microsc 172:177–180
21. Iwahashi H, Eguchi Y, Yasuhara N, Hanafusa T, Matsuzawa Y, Tsujimoto Y (1997) Synergistic antiapoptotic activity between bcl-2 and SMN implicated in spinal muscular atrophy. Nature 390:413–417
22. Kerr DA, Nery JP, Traystman RJ, Chau BN, Hardwick JM (2000) Survival motor neuron protein modulates neuron-specific apoptosis. Proc Natl Acad Sci USA 97:13312–13317
23. Kesari A, Idris MM, Chandak GR, Mittal B (2005) Genotype– phenotype correlation of SMN locus genes in spinal muscular atrophy patients from India. Exp Mol Med 37:147–154
24. Kimura T, Budka H (1984) Glial bundles in spinal nerve roots. An immunocytochemical study stressing their nonspecificity in various spinal cord and peripheral nerve diseases. Acta Neuropathol 65:46–52
25. Kozlowski MA, Williams C, Hinton DR, Miller CA (1989) Heterotopic neurons in spinal cord of patients with ALS. Neurology 39:644–648
26. Lefebvre S, Burglen L, Reboullet S, Clermont O, Burlet P, Viollet L, Benichou B, Cruaud C, Millasseau P, Zeviani M, Le Paslier D, Fre´zal J, Cohen D, Weissenbach J, Munnich A, Melki J (1995) Identification and characterization of a spinal muscular atrophy-determining gene. Cell 80:155–165
27. Lind D, Franken S, Kappler J, Jankowski J, Schilling J (2005) Characterization of the neuronal marker NeuN as a multiply phosphorylated antigen with discrete subcellular localization. J Neurosci Res 79:295–302
28. Lorson CL, Strasswimmer J, Yao J-M, Baleja JD Hahnen E, Wirth B, Le T, Burghes AH, Androphy EJ (1998) SMN oligomerization defect correlates with SMA severity. Nat Genet 19:63–66
29. Lorson CL, Hahnen E, Androphy EJ, Wirth B (1999) A single nucleotide in the SMN gene regulates splicing and is responsible for spinal muscular atrophy. Proc Natl Acad Sci 96:6307–6311
30. Lucassen PJ, Chung WCJ, Vermeulen JP, Van Lookeren Campagne M, Van Dierendonck JH, Swaab DF (1995) Microwaveenhanced in situ end-labeling of fragmented DNA: parametric studies in relation to post mortem delay and fixation of rat and human brain. J Histochem Cytochem 43:1163–1171
31. Mailman MD, Heinz JW, Papp AC, Snyder PJ, Sedra MS, Wirth B, Burghes AH, Prior TW (2002) Molecular analysis of spinal muscular atrophy and modification of the phenotype by SMN2. Genet Med 4:20–26

32. Marschall A, Duchen LW (1975) Sensory system involvement in infantile spinal muscular atrophy. J Neurol Sci 26:349–359
33. Martin JE, Mather K, Swash M (1993) Heterotopic neurons in amyotrophic lateral sclerosis. Neurology 43:1420–1422
34. McWhorter ML, Monani UR, Burghes AH, Beattie CE (2003) Knockdown of the survival motor neuron (Smn) protein in zebrafish causes defects in motor axon outgrowth and pathfinding. J Cell Biol 162:919–931
35. Monani UR, Lorson CL, Parsons DW, Prior TW, Androphy EJ, Burghes AH, McPherson JD (1999) A single nucleotide difference that alters splicing patterns distinguishes the SMA gene SMN1 from the copy gene SMN2. Hum Mol Genet 8:1177–1183
36. Oskoui M, Levy G, Garland CJ, Gray JM, O0Hagen J, De Vivo DC, Kaufmann P (2007) The changing natural history of spinal muscular atrophy type 1. Neurology 69:1931–1936
37. Pagliardini S, Giavazzi A, Setola V, Lizier C, Di Luca M, DeBiasi S, Battaglia G (2000) Subcellular localization and axonal transport of the survival motor neuron (SMN) in the developing rat spinal cord. Hum Mol Genet 9:47–56
38. Parsons DW, McAndrew PE, Iannaccone ST, Mendell JR, Burghes AH, Prior TW (1998) Intragenic telSMN mutations: frequency, distribution, evidence of a founder effect, and modification of the spinal muscular atrophy phenotype by cenSMN copy number. Am J Hum Genet 63:1712–1723
39. Rossoll W, Jablonka S, Andreassi C, Kroning AK, Karle K, Monani UR, Sendtner M (2003) Smn, the spinal muscular atrophy-determining gene product, modulates axon growth and localization of beta-actin mRNA in growth cones of motoneurons. J Cell Biol 163:801–812
40. Roy N, Mahadevan MS, McLean M, Shutler G, Yaraghi Z, Farahani R, Baird S, Besner-Johnston A, Lefebvre C, Kang X, Salih M, Aubry H, Tamai K, Guan X, Ioannou P, Crawford TO, de Jong PJ, Surh L, Ikeda JE, Korneluk RG, MacKenzie A (1995) The gene for neuronal apoptosis inhibitory protein is partially deleted in individuals with spinal muscular atrophy. Cell 80:167–178
41. Sasaki S, Iwata M (2004) Characterization of heterotopic neurons in the spinal cord of amyotrophic lateral sclerosis patients. Acta Neuropathol 95:367–372
42. Sato K, Eguchi Y, Kodama TS, Tsujimoto Y (2000) Regions essential for the interaction between Bcl-2 and SMN, the spinal muscular atrophy disease gene product. Cell Death Differ 7:374–383
43. Scharf JM, Endrizzi MG, Wetter A, Huang S Thompson TG, Zerres K, Dietrich WF, Wirth B, Kunkel LM (1998) Identification of a candidate modifying gene for spinal muscular atrophy by comparative genomics. Nat Genet 20:83–86
44. Selig S, Bruno S, Scharf JM, Wang CH Vitale E, Gilliam TC, Kunkel LM (1995) Expressed cadherin pseudogenes are localized to the critical region of the spinal muscular atrophy gene. Proc Natl Acad Sci 92:3702–3706
45. Sertić J, Barišić N, Šoštarko M, Bošnjak N, Čulić V, Cvitanović L, Ferenčak G, Brzović Z, Stavljenić-Rukavina A (1997) Deletions in the SMN and NAIP genes in patients with spinal muscular atrophy in Croatia. Coll Antropol 21:487–492
46. Setola V, Terao M, Locatelli D, Bassanini S Garattini E, Battaglia G (2007) Axonal-SMN (a-SMN), a protein isoform of the survival motor neuron gene,

is specifically involved in axonogenesis. Proc Natl Acad Sci USA 104:1959–1964
47. Shishikura K, Hara M, Sasaki Y, Misugi K (1983) A neuropathologic study of Werdnig–Hoffmann disease with special reference to the thalamus and posterior roots. Acta Neuropathol 60:99–106
48. Šimić G, Šešo-Šimić Đ, Lucassen P, Islam A, Krsnik Z, Cviko A Jelašić D, Barišić N, Winblad B, Kostović I, Krušlin B (2000) Ultrastructural analysis and TUNEL demonstrate motor neuron apoptosis in Werdnig–Hoffmann disease. J Neuropathol Exp Neurol 59:398–407
49. Veldink JH, Kalmijn S, Van der Hout AH, Lemmink HH, Groeneveld GJ, Lummen C, Scheffer H, Wokke JH, Van den Berg LH (2005) SMN genotypes producing less SMN protein increase susceptibility to and severity of sporadic ALS. Neurology 65:820–825
50. Werdnig G (1981) Zwei fru¨hinfantile heredita¨re Fa¨lle von progressiver Muskelatrophie unter dem Bilde der Dystrophie, aber auf neurotischer Grundlage. Arch Psychiatr Nervenkr 22:437–481
51. Wharton S, Ince PG (2003) Pathology of motor neuron disorders. In: Shaw PJ, Strong MJ (eds) Motor neuron disorders. Blue books of practical neurology, book 28. Butterworth-Heineman, Elsevier Science, Philadelphia, pp 17–49
52. Wijsman JH, Jonker RR, Keijzer R, Van de Velde CJH, Cornelisse CJ, Van Dierendonck JH (1993) A new method to detect apoptosis in paraffin sections: in situ end labeling of fragmented DNA. J Histochem Cytochem 41:7–12
53. Young P, Le TT, Dunckley M, Nguyen TM, Burghes AH, Morris GE (2001) Nuclear gems and Cajal (coiled) bodies in fetal tissues: nucleolar distribution of the spinal muscular atrophy protein, SMN. Exp Cell Res 265:252–261
54. Young PJ, Day PM, Androphy EJ, Morris GE, Lorson CL (2002) A direct interaction between survival motor neuron protein and p53 and its relationship to spinal muscular atrophy. J Biol Chem 277:2852–2859

Figure legends

Fig. 1 (a) Abnormally heterotopic (migratory) motoneurons (HMN) can be found in SMA subjects all along the ‘‘ventral outflow,’’ from the anterior horn (AH) to the ventral root (VR). Cresyl-violet stain. (b) Higher magnification of the frame in a. Heterotopic neurons were always undifferentiated (oval shaped), without visible axon and dendrites. Cresyl-violet stain. (c) A chromatolytic (ballooned) motoneuron (bmn) from the gray matter of AH of the same SMA-I subject for comparison with b. Note the well-developed neuronal processes (arrows). Cresyl-violet stain. Scale bars: (a) 200 µm; (b, c) 20 µm

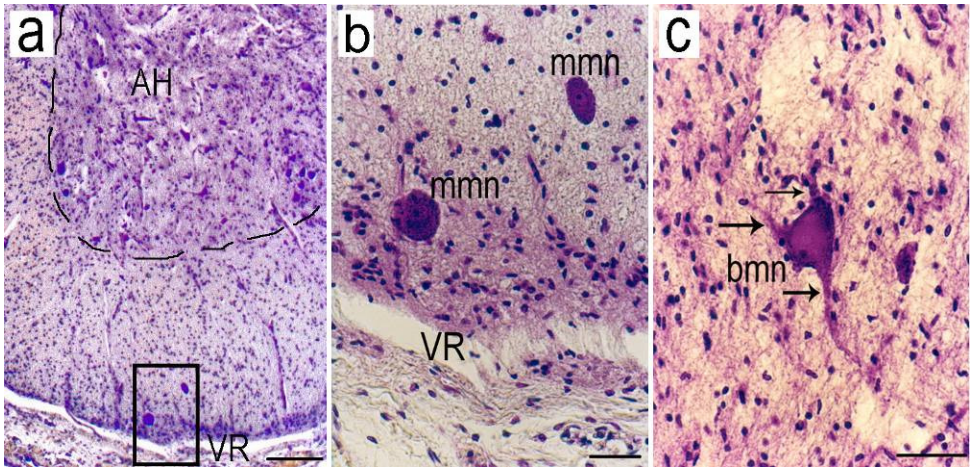

Fig. 2 (a, b) Accumulation of heterotopic (migratory) motoneurons (HMN, mmn) at the anterior rim of the spinal cord. AH, anterior horn, VR, ventral root. Cresyl-violet stain. (a) Female five-month-old SMA-I subject. (b) Male eightmonth- old SMA-I subject. (c) In some sections, particularly those of younger SMA-I subjects, we observed more than 10 heterotopic motoneurons ‘‘aligned’’ at the front wall of the spinal cord (lower left corner arrow) or outside the spinal cord (lower right corner arrow). Scale bars = 20 μm

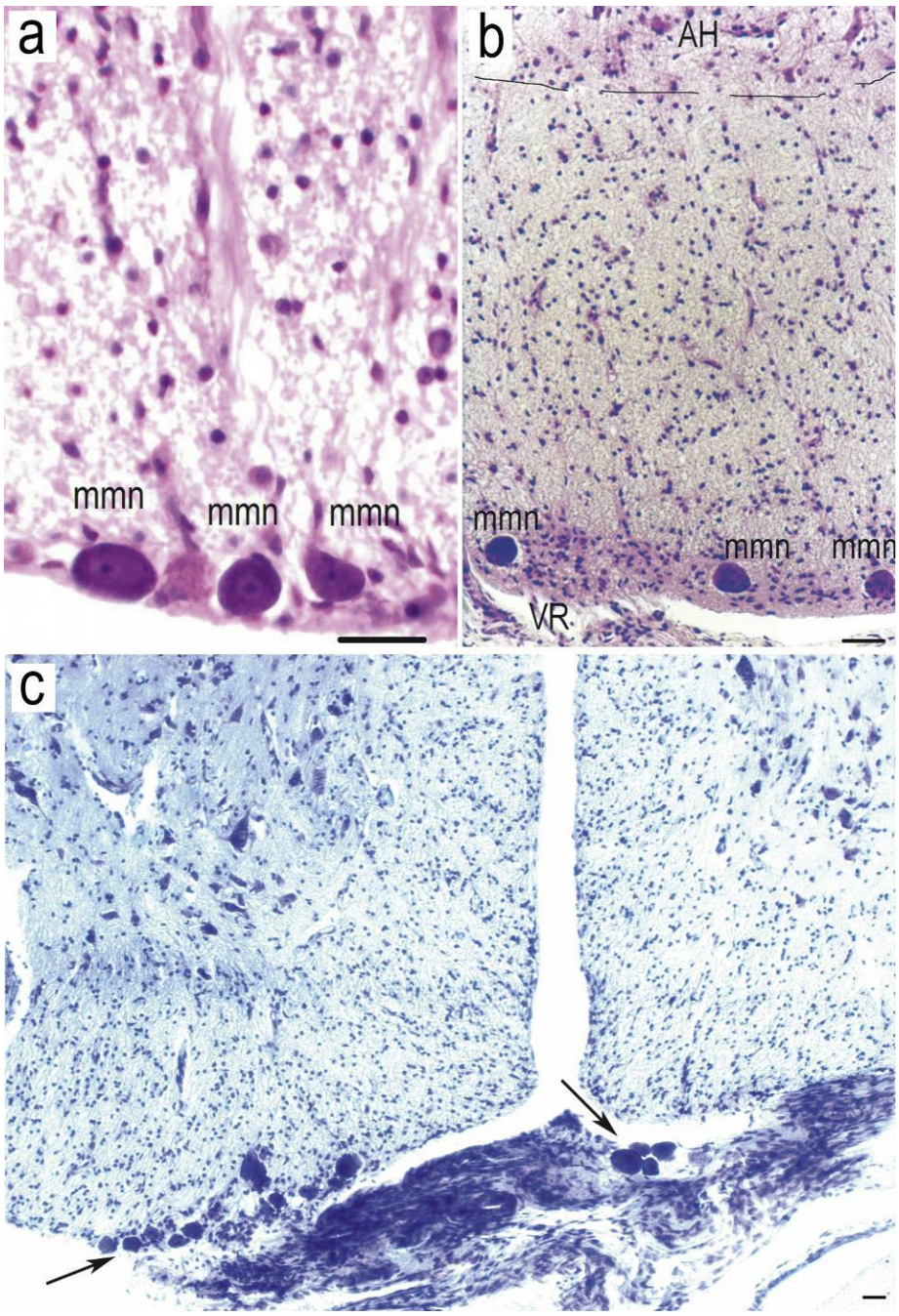

Fig. 3 (a) Two oval-shaped hyperchromatic heterotopic (migratory) motoneurons (HMN, mmn) at the anterior rim of the spinal cord of SMA-I subject. VR, ventral root; AH, anterior horn. Cresyl-violet stain. (b) Higher magnification of the frame in a. Note activated microglial cells around and ‘‘behind’’ (i.e., along the migrational route) the heterotopic motoneurons (arrows). Cresyl-violet stain. (c, d, e) Neuronophagia of heterotopic motoneurons by glial cells. Cresyl-violet stain. Scale bars: (a) 200 μm; (b–e) 20 μm

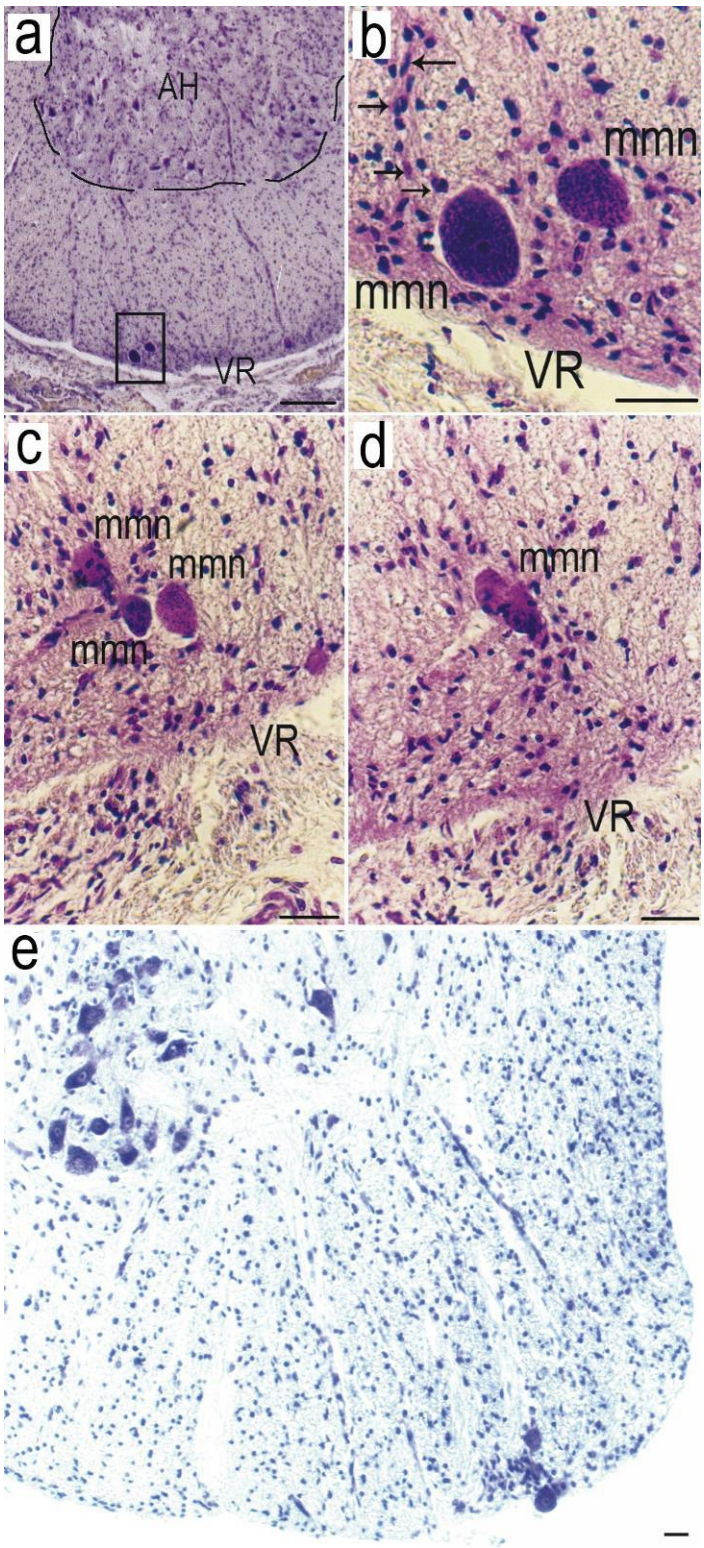

Fig. 4 (a) Two wandering motoneurons making their way out of the spinal cord and three more at the anterior rim of the spinal cord of a child with SMA-I. VR, ventral root, AH, anterior horn. Cresyl-violet stain. (b) Higher magnification of the frame in a. (c) Pronounced neuronophagia of heterotopic motoneurons (arrows), particularly within the ventral spinal root (VR) of a SMA-I subject. Cresyl-violet stain. (d) Detached ventral root (VR) containing three heterotopic (migratory) motoneurons (HMN, mmn) within glial cell bundles (GB). (e) Five HMN, two of which seem to degenerate (arrows). Cresyl-violet stain. Scale bars: (a) 200 µm; (b–e) 20 µm

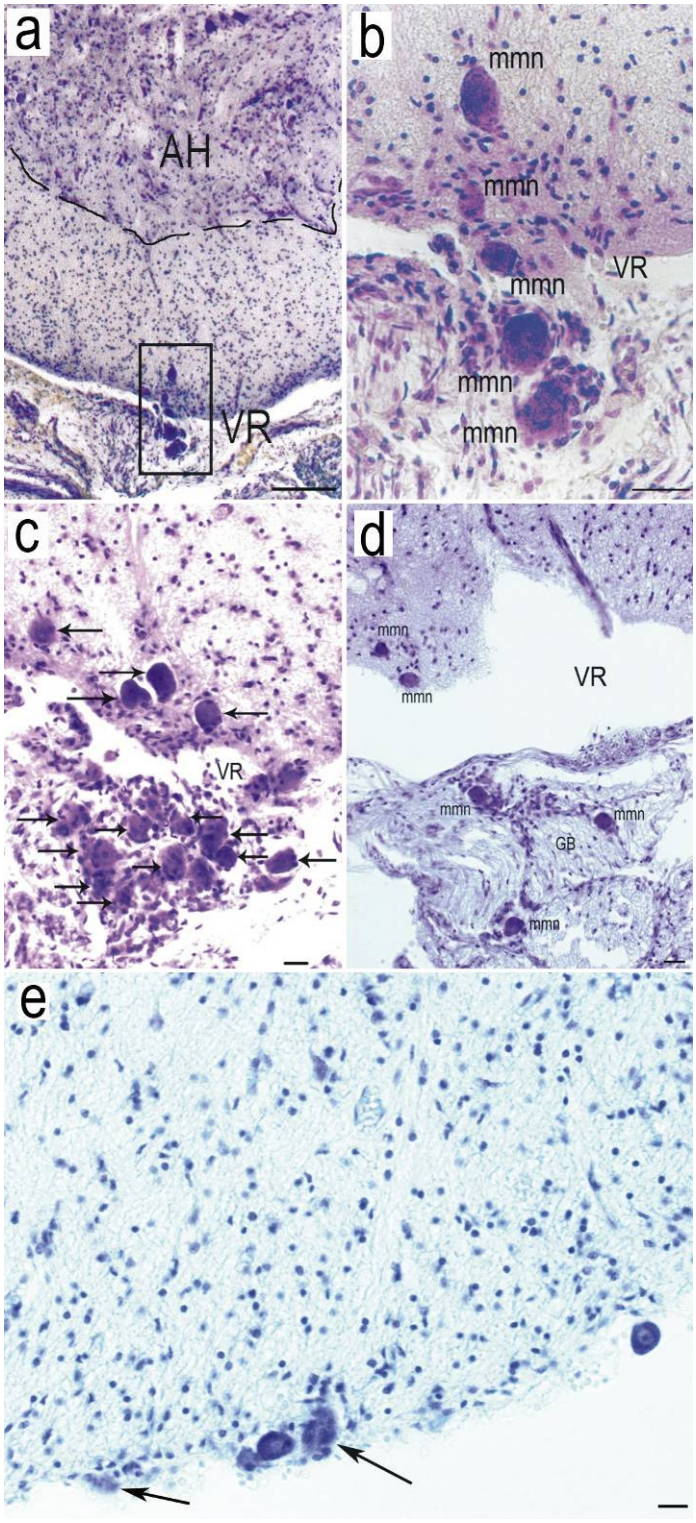

Fig. 5 (a) Two abnormally migrating cells (arrows) dorsal to the thoracic nucleus (NT, Clarke's column) in a SMA subject. (b) Higher magnification of the frame in a. (c, d) Relatively welldifferentiated Heterotopic neurons in the ''dorsal outflow'' (arrows). Cresyl-violet stain. Scale bars: (a–d) 200 μm

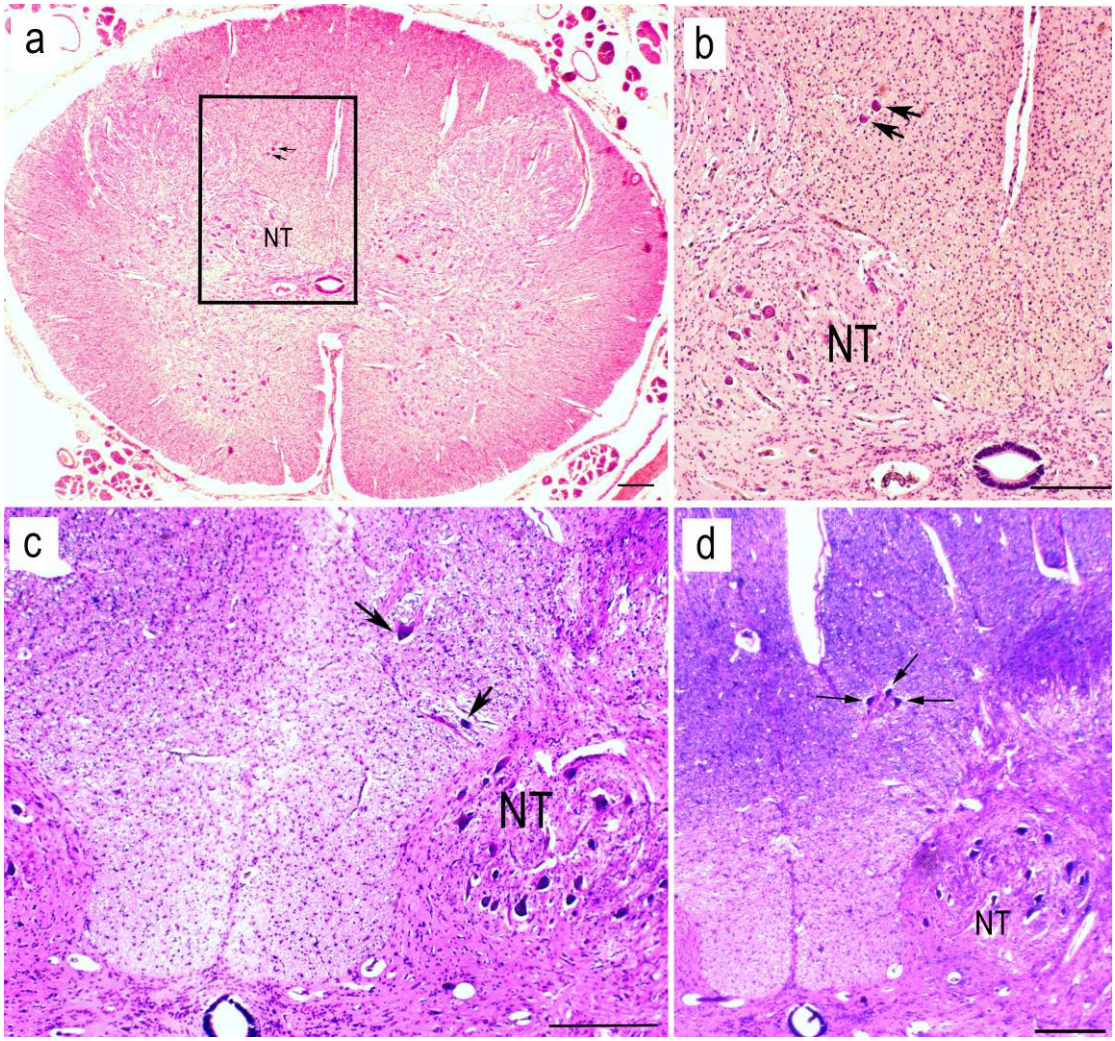

Fig. 6 NeuN immunocytochemistry of several SMA-I and SMA-II subjects (a–f). Note that all slides were prestained by cresyl-violet (therefore, some of the cells, mostly ependymal glial cells around the central canal remained filled with cresyl-violet and have a purple color, identifiable from the specific NeuN staining visualized by DAB (dark brown to black color). About a half of heterotopic motoneurons at the anterior rim of the spinal cord were NeuN-positive (arrows), the other half were not (arrowheads). Scale bars: 200 μm

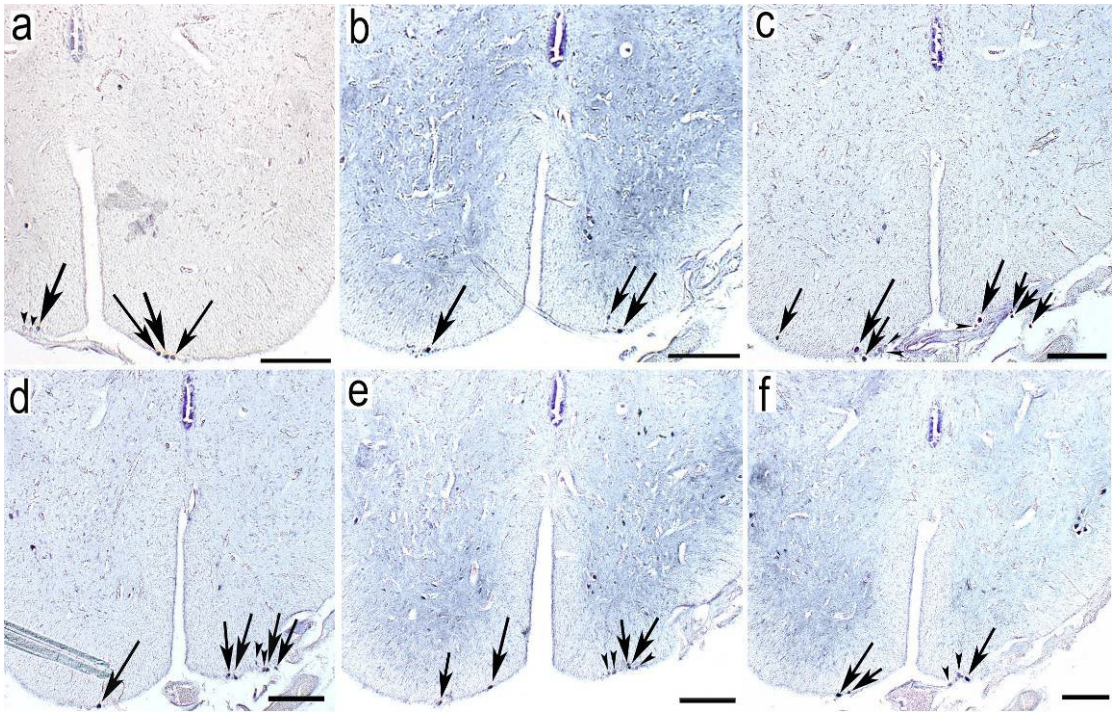

Fig. 7 MAP-2 immunocytochemistry of two SMA-I cases (a–e) and one control (f). Panel b shows the upper inset from a and shows two MAP2-positive (dark-brown DAB product) neurons within anterior horn (arrows), c is lower inset from a and shows five MAP2-negative heterotopic neurons (arrowheads); one more is illustrated in e (arrowhead). Arrows in d show four MAP2-positive HMN. Summarizing all analyzed slides from eight SMA subjects together, only about 1/3 of the observed HMN were positive for MAP2 protein. Scale bars: (a, d, e) 500 µm; (b, f) 50 µm; (c) 100 µm

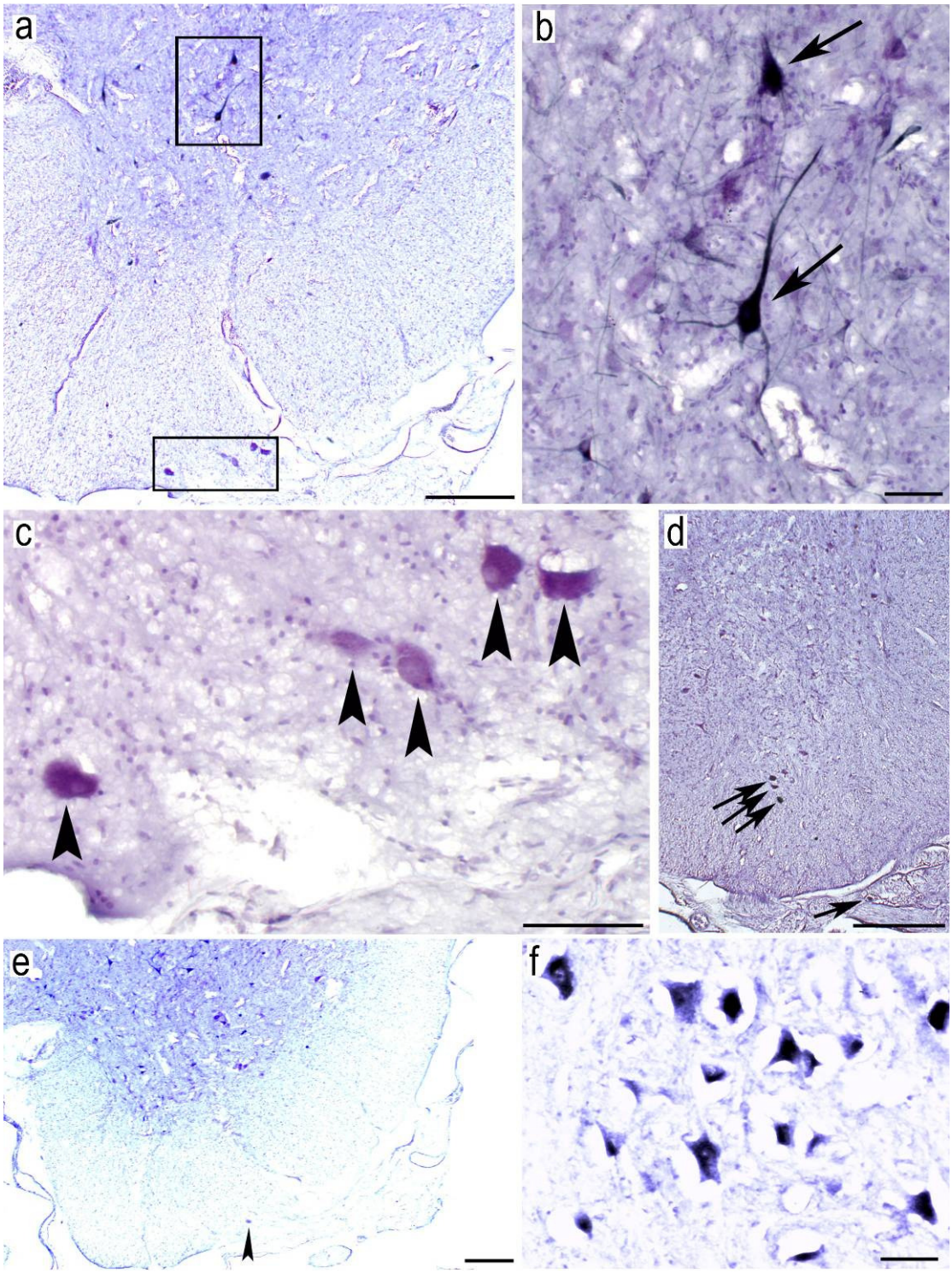

Fig. 8 CD68 immunohistochemistry. (a) Nissl stain of several HMN before CD68 immunohistochemistry. (b) Same slide after CD68 immunohistochemistry. Several CD68 immunoreactive activated microglial cells in the vicinity of HMN at the anterior rim of the spinal cord of SMA subject are shown by arrows. (c, e) Two representative pictures of CD68-positive microglial cells. Arrows in c show three microglial cells attached to heterotopic (migratory) motoneuron. (d) Inset of c, a microglial cell (arrowhead) better seen in another optical plane. Arrowheads in e show several CD68-positive microglia cells along the migrational route of HMN. (f) Heterophagic elimination of HMN by several CD68-positive activated microglial cells. Note disintegration of HMN and loss of tigroid substance (rough endoplasmic reticulum). (g) Control spinal cord. Only CD68-positive microglia associated with blood vessels could be occasionally seen (arrowhead). (h) Positive control showing many CD68-positive activated microglial cells (rat prostate). Scale bars = 20 μm

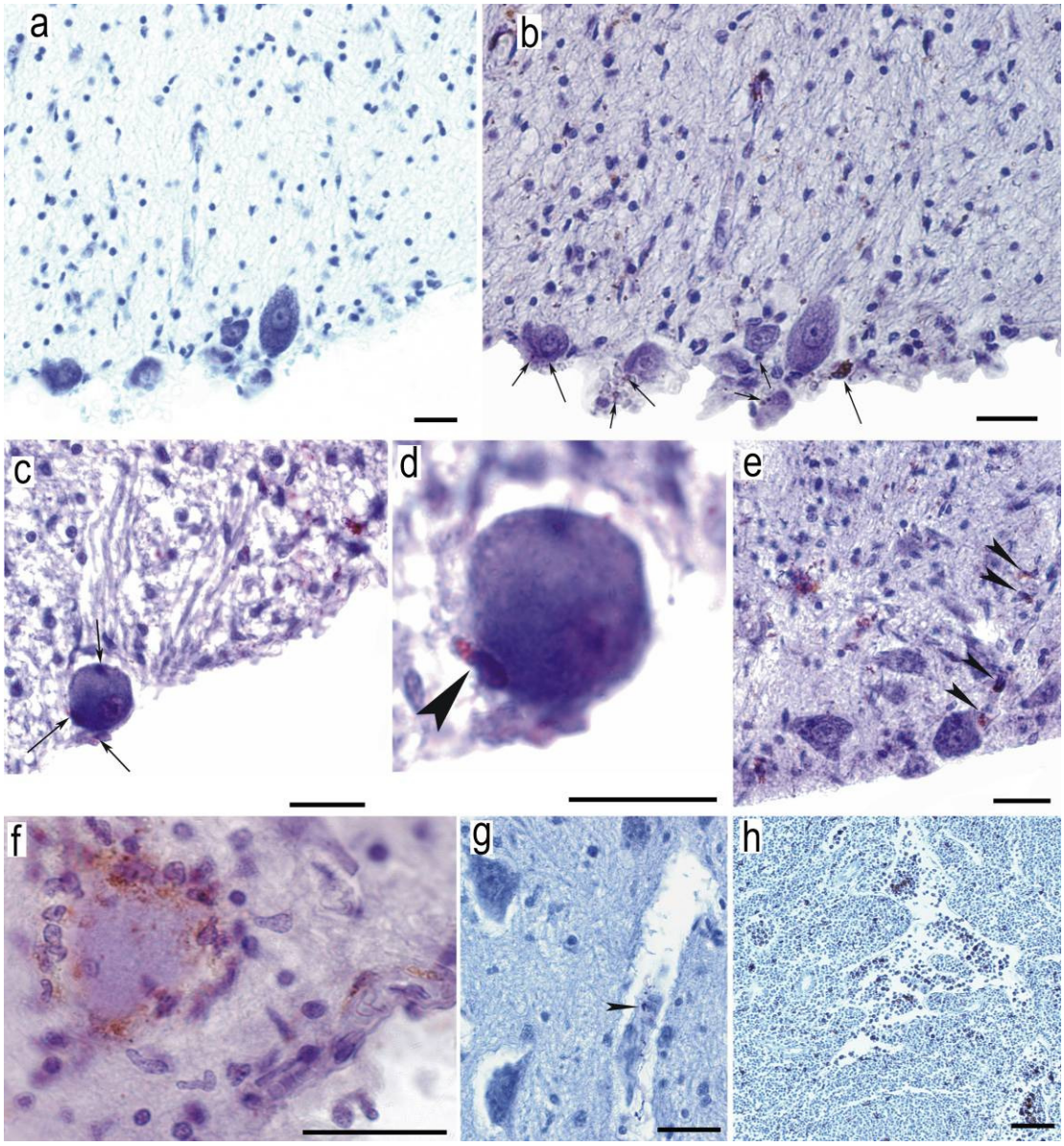

Fig. 9 In situ end-labeling (ISEL). Sections are lightly counterstained with methyl green. Control sections of spinal cord had no ISEL-positive cells, except occassional vascular microglia (not shown). Although activation of microglial cells was more frequently seen within the anterior horns of SMA patients, where ISEL-positive microglia phagocytized apoptotic and degenerating motoneurons (a and b), ISEL-positive microglia were also seen in the anterior white matter of SMA subjects. Apoptosis of these microglial cells is probably associated with their demise upon elimination of HMN (c). Small arrowheads show ISEL-positive microglia, large arrowheads show ISEL-positive neurons. Note that ISEL labeling of microglial nuclei is often more intensive than of the cytoplasm, e.g., ISELpositive microglial cell in the lower right corner in a. (d) ISELpositive necrotic HMN at the anterior rim of the spinal cord of SMA-I subject. (e) inset from d at higher magnification. This was a relatively rare finding since most of the HMN were looking morphologically healthy and were not ISEL-positive. (f) Immunoreactivity for GFAP showed large inter- and intrasubject variability in SMA patients. The anterior horns were however consistently more immunoreactive for GFAP than posterior horns, as shown in f. In contrast to controls, where GFAP immunoreactivity consisted of lightly and evenly distributed immunoreactivity of small astrocytes within the white matter fiber tracts, many sections from SMA subjects revealed the presence of medium and large astrocytes in close proximity to ‘‘empty cell beds’’ within the ventral horns of the spinal cord (g). Subjects who died at an older age had high numbers of GFAP-positive astrocytes (h, not quantified). We found no GFAP-positive astroglia around HMN (i). AH, anterior horn; VR, ventral root. Scale bars: (a, b, e, h, i) 20 μm; (c, d, f) 200 μm; (g) 10 μm

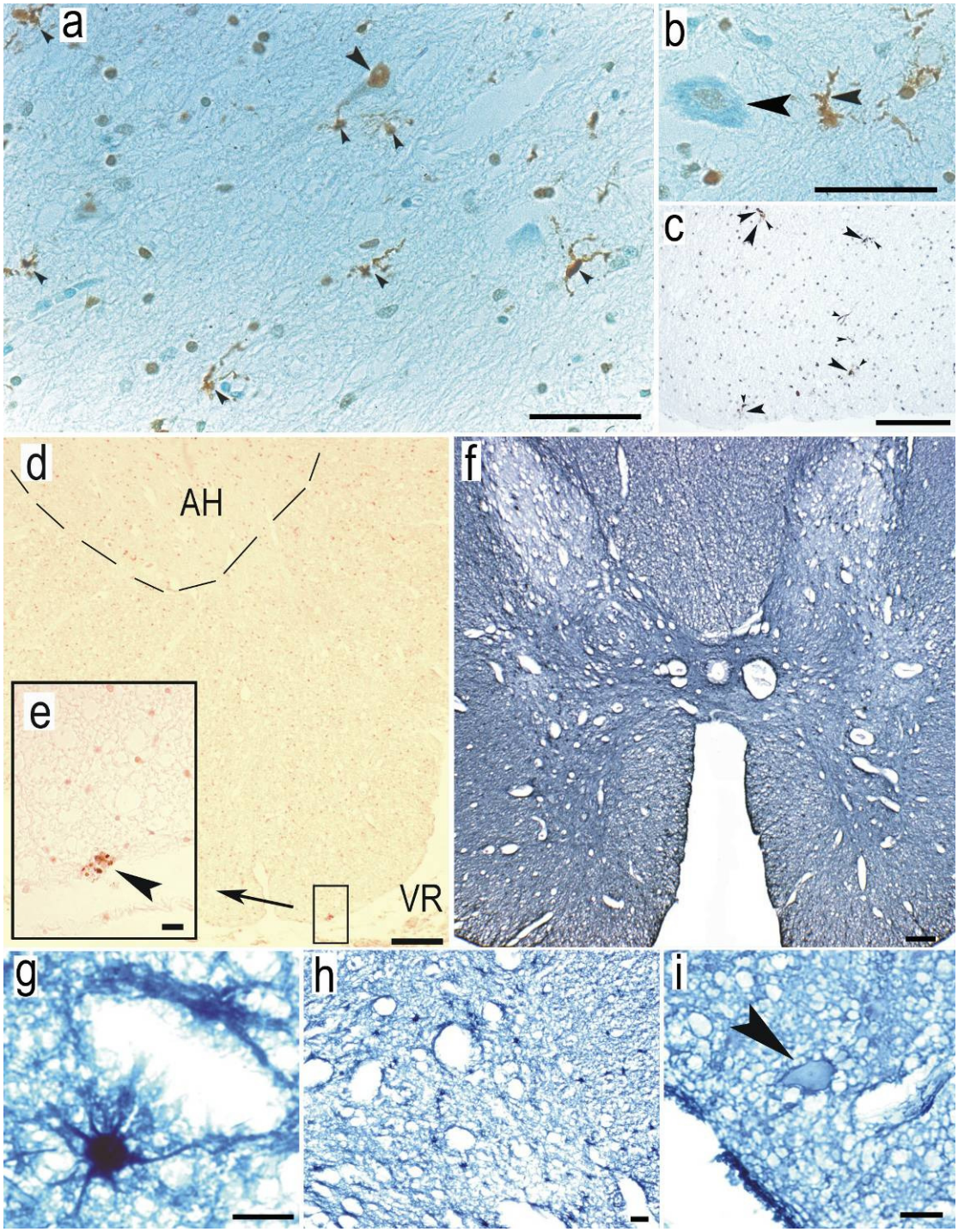
a
b
c
d
AH
e
VR
f
g
h
i

Fig. 10 (a) Electron microscopic appearance of a heterotopic motoneuron. Ultrastructural changes include breakdown of the plasma membrane, dilation and vacuolization of cytoplasmic organelles and loss of structure, which are all consistent with necrotic cell death (type 3b according to classification of Clarke [9]). In contrast to normal motoneurons, heterotopic motoneurons contained no identifiable synapses. In the lower left corner is an apoptotic microglial cell (arrow), as judged from its small size and clumping of the chromatin along the inner side of the nuclear envelope. (b) Another heterotopic motoneuron in relatively late stage of necrotic degeneration with dilation and rupture of most of the cytoplasmic organelles. Arrow shows an apoptotic microglial cell in the lower right corner. Scale bars: (a, b) 1 μm

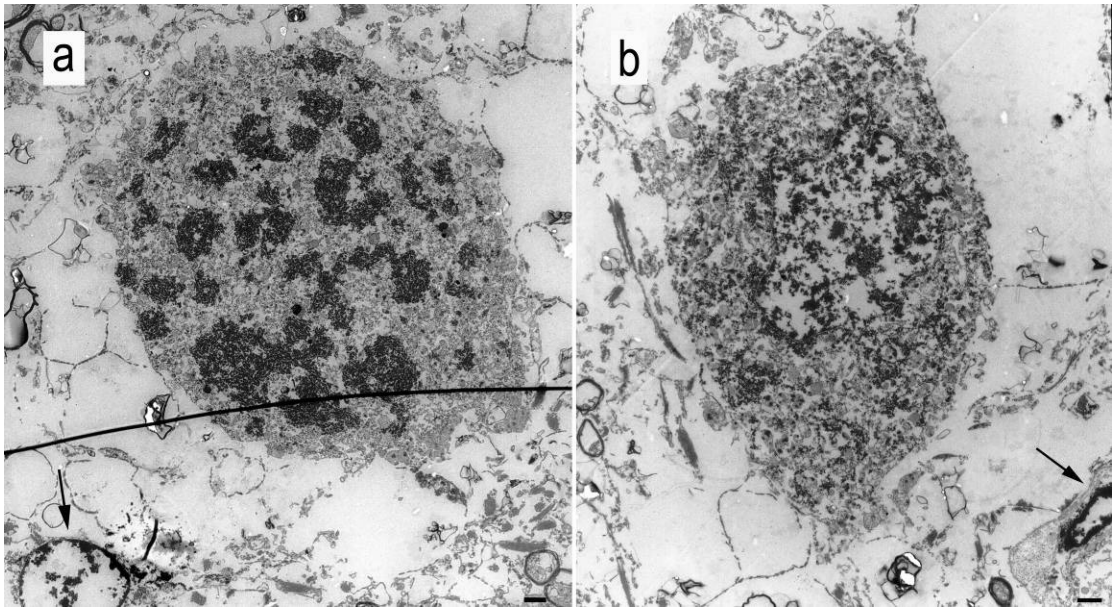

Fig. 11 Number of heterotopic motoneurons found in the spinal cords of six SMA-I (circles) and two SMA-II subjects (squares). There was a statistically significant negative correlation between thenumber of heterotopic neurons and age (r = -0.64, p=0.04)